ISSN 1070-3284, Russian Journal of Coordination Chemistry, 2015, Vol. 41, No. 10, pp. 706–714. © Pleiades Publishing, Ltd., 2015.

Synthesis and Structural Determination of Polynuclear Nine-Coordinate $\{K[Sm^{III}(Egta)] \cdot H_2O\}_n$ and Mononuclear Eight-Coordinate $(NH_4)[Lu^{III}(Egta)] \cdot H_2O$[1]

B. Li, F. Y. Tian, C. Qin, D. Y. Kong, and J. Wang*

Department of Chemistry, Liaoning University, Shenyang, 110036 P.R. China

**e-mail: wangjuncomplex890@126.com*

Received January 24, 2015

Abstract—Two novel rare earth metal coordination compounds, $\{K[Sm^{III}(Egta)] \cdot H_2O\}_n$ (**I**) (H_4Egta = ethyleneglycol-*bis*(2-aminoethylether)-N,N,N',N'-tetraacetic acid) and $(NH_4)[Lu^{III}(Egta)] \cdot H_2O$ (**II**), have been successfully synthesized through direct heating reflux and characterized by FT-IR spectroscopy, thermal analysis and single-crystal X-ray diffraction techniques (CIF file CCDC nos. 966211 (**I**) and 966210 (**II**)). Complex I shaps a polynuclear and nine-coordinate structure with distorted monocapped square antiprismatic (MC-SAP) conformation and crystallizes in the monoclinic crystal system with space group $C2/c$. The central Sm^{3+} ion is coordinated by two nitrogens and six oxygens from one octadentate Egta ligand. Meanwhile, one oxygen atom comes from one carboxylic group of the neighboring Egta ligand, forming one dimensional unlimited polynuclear complexes. The cell dimensions are: a = 38.253(3), b = 13.7769(11), c = 8.7652(7) Å, β = 100.696(2)° and V = 4539.0(6) Å^3. Complex (II) adopts a mononuclear structure with eight-coordinate pseudo-SAP conformation and crystallizes in the monoclinic crystal system with space group $P2_1/c$. The central Lu^{3+} ion is coordinated by two nitrogens and six oxygens all from one octadentate Egta ligand. The crystal data are as follows: a = 13.9817(10), b = 9.7392(6), c = 14.6305(13) Å, β = 110.267(9)° and V = 1868.9(2) Å^3.

DOI: 10.1134/S1070328415100036

INTRODUCTION

In the past decades, a growing interest in study of lanthanide(III) complexes have increasingly been a research focus. Lanthanide(III) complexes play an important role in different multidisciplinary area [1, 2]. The prospective implementations of them is determined by not only special physical and chemical properties of rare earth elements, but also their rich coordination structures [3]. For example, the attractive applications of Gd^{III} complexes as shift reagents for nuclear magnetic resonance spectroscopy and relaxation contrast reagents owing to their large magnetic moment and relatively low toxicity [4, 5]. The Tb(III) and Eu(III) complexes exhibit unusual spectroscopic characteristics with narrow linewidths and long luminescence decay times, making for a high "color purity" of the emitted light. It is potentially favourable for many applications, such as fluorescence probes for medical diagnostics, light emitting diode (LED), biological sensors, fluoroimmunoassays, lasers materials, electroluminescent devices, etc. [6–9]. In particular, the therapeutic applications of ^{153}Sm complexes are valuable in nuclear medicine area due to their moderate decay properties [10, 11]. What's more, ^{153}Sm complexes with phosphonate groups in ligands have showed good function for bone pain relief and treatment of bone metastasis in clinical [12]. Among the lanthanide series, Lu^{+3} ion is the last one and has a minimum radius (0.98 Å). Lutetium has a wide range of applications in our daily life, it is everywhere around us, it can be found in some equipments such as color televisions, glasses, fluorescent lamps and energy-saving lamps, etc. [13]. Lutetium phthalocyanines have been studied due to their electrochromic properties and high intrinsic conductivity. The Lu(III) complexes can be used in many research fields especially in electrochromic applications and antineoplastic pharmaceutical field [14, 15]. According to recent clinical trials, (^{177}Lu-dota-tyr^3)-octreotide (known as ^{177}Lu-dota-toc) and (^{177}Lu-dota-tyr^3)-octreotate (known as ^{177}Lu-dota-tate) have been reported have high-efficiency and long-lasting on the treatment for those patients who suffered from different types of neuroendocrine tumors [16]. In general, many radioactive rare earth metal ions such as ^{86}Y(III), ^{149}Pm(III), ^{153}Sm(III), ^{166}Ho(III), and ^{172}Lu(III) can emit radiation and their complexes are investigated to diagnose and treat various tumors because of their appropriate half-life and energy. For example, ^{153}Sm(III)-EDTMP, ^{166}Ho(III) -EDTMP, ^{177}Lu(III)-EDTMP (EDTMP = ethylenediamine-N,N,N',N'-tetramethylenephosphonate) have been tested and

[1] The article is published in the original.

applied for human studies. What's more, they are often used in radiotherapy of bone metastases [17]. But we don't expect that these treatment medicines or clinical diagnosis drugs still stay in the patient's body chronically after completing the therapy or diagnosis. So, it is necessary to find out stable and non-toxic chelating agents that can combine with rare earth metal ions as stable complexes and safely and effectively delivered them in the human body. Among all sorts of ligands, aminopolycarboxylic acids are usually considered as fascinating one, which been chosen in the construction of lanthanide complexes. Meanwhile, according to some preclinical trials, polyaminocarboxylic acids offen used in nuclear medicine preclinical trials for radioimmunotherapy applications as chelating agents. These complexes could enter into the body as stable complexes without harmful effects, and have high-affinity and selectivity on the focus position and quickly be cleared from the body after the diagnosis or treatment [18]. Therefore, it is necessary to study constructions of lanthanide complexes in order to help us to come to a better understanding of their applications.

Although, rare earth metal ions have similar radius size, however, several years effort of synthesis and determination of rare earth metal complexes with ligands containing aminopolycarboxylic acids proves that coordination number and conformation of these complexes are rich and diverse. In general, rare earth metal ions are easy to form high-coordinate complexes with relatively more orbital electrons in f-orbital. In other respect, it is easy to form low-coordinate complex with relatively small orbital electrons in f-orbital. Therefore, for these rare earth metal ions with relatively larger radius (La(III), Ce(III), Pr(III) and Nd(III)), they always tend to form ten-coordinate or nine-coordinate complexes. For those in the middle of lanthanide series (Pm(III), Sm(III), Eu(III), Gd(III), Td(III), Dy(III), Ho(III) and Er(III)), they always intend to form nine-coordinate or eight-coordinate complexes. For these rare earth metal ions with relatively smaller radius (Tm(III), Yb(III) and Lu(III)), they are tend to form eight-coordinate complexes.

In recent years, our laboratory have reported a series of lanthanide(III) complexes with H_4Egta ligands (H_4Egta = ethyleneglycol-*bis*(2-aminoethyl-ether)-N,N,N',N'-tetraacetic acid), such as $(EnH_2)[Sm^{III}(Egta)(H_2O)]_2 \cdot 6H_2O$ [19], $(MnH)_2[Eu^{III}(Egta)]_2 \cdot 6H_2O$ [20], $(EnH_2)[Gd^{III}(Egta)(H_2O)]_2 \cdot 6H_2O$ [21], $(EnH_2)[Er^{III}(Egta)(H_2O)]_2 \cdot 6H_2O$ [22], $\{K[Y^{III}(Egta) \cdot 4H_2O\}_n$ [23] and $(EnH_2)[Ho^{III}(Egta)(H_2O)]_2$ [24]. It was found that these complexs can adopt mononuclear eight or nine coordinate structure with the pseudo-monocapped square antiprismatic (**MC-SAP**) and pseudo-SAP in geometry. Meanwhile, they can also adopt polynuclear nine-coordinate with MC-SAP. However, it is noteworthy that there is no binuclear coordinate structure complex among them. We learn from inherent laws and experiences that geometrical conformation and coordination number of lanthanide complexes are relate to its rare earth metal ionic radius, electronic configuration, different kinds of counter cations, as well as shape of ligands [25]. Based on past experience, we predicted the Sm(III) complex with Egta ligands and counter cations (K^+) perhaps forms polynuclear nine-coordinate structure. For Lu(III) complexes, Lu^{+3} ion has minimum ionic radius (0.98 Å) among the rare earth metal ions and high-spin electronic configurations f^{14}, making it possible to form low-coordinate complexes. So, we predicted that the Lu(III) complex with Egta ligands and counter cations (NH_4^+) should adopt a eight-coordinate structure. However, we still want to know how different sizes of rare earth metal ionic radius and counter cation species affect the coordination number, coordinate structure, space group, molecular structure and crystal structure.

In order to extend our research and verify our guess, aminopolycarboxylic acids (for example, H_4Egta) were chosen as ligand, K^+ and NH_4^+ were chosen as counter cations, respectively. Two novel rare earth metal complexes with aminopolycarboxylic acid ligands, namely, $\{K[Sm^{III}(Egta)] \cdot H_2O\}_n$ (**I**) and $(NH_4)[Lu^{III}(Egta)] \cdot H_2O$ (**II**), were successfully synthesized. Consequently, as we predicted, complex **I** adopts a polynuclear and nine-coordinate structure with distorted MC-SAP and crystallizes in the monoclinic crystal system with space group $C2/c$. Meanwhile, complex II displays a mononuclear eight-coordinate structure due to its different center of metal ions and nature of counter cations. We testified our analysis through this fact, so we can safely draw a conclusion that the ionic radius, counter cations and ligand structures are of vital importance on the coordinate structure of lanthanide metal complexes.

EXPERIMENTAL

Materials and methods. Sm_2O_3 powder (99.999%, Yuelong Rare Earth Co., Ltd., China), Lu_2O_3 powder (99.999%, Yuelong Rare Earth Co., Ltd., China) and ligand of H_4Egta (A.R., Beijing SHLHT Science and Trade Co., Ltd., China) were used to synthesize the title aminopolycarboxylic acid complexes. In addition, $KHCO_3$ aqueous solution and NH_3 aqueous solution were slowly added to above solution in order to adjust the pH to 5.5. The structures of complexes were detected by X-ray equipment (XT-V130, Beijing Xinzhuo, Company, China).

Synthesis of I. H_4Egta (A.R., Beijing SHLHT Science and Trade Co., Ltd., China) (1.9017 g, 5.0 mmol) was added to 100 mL warm water and Sm_2O_3 powder (99.999%, Yuelong Rare Earth Co.,

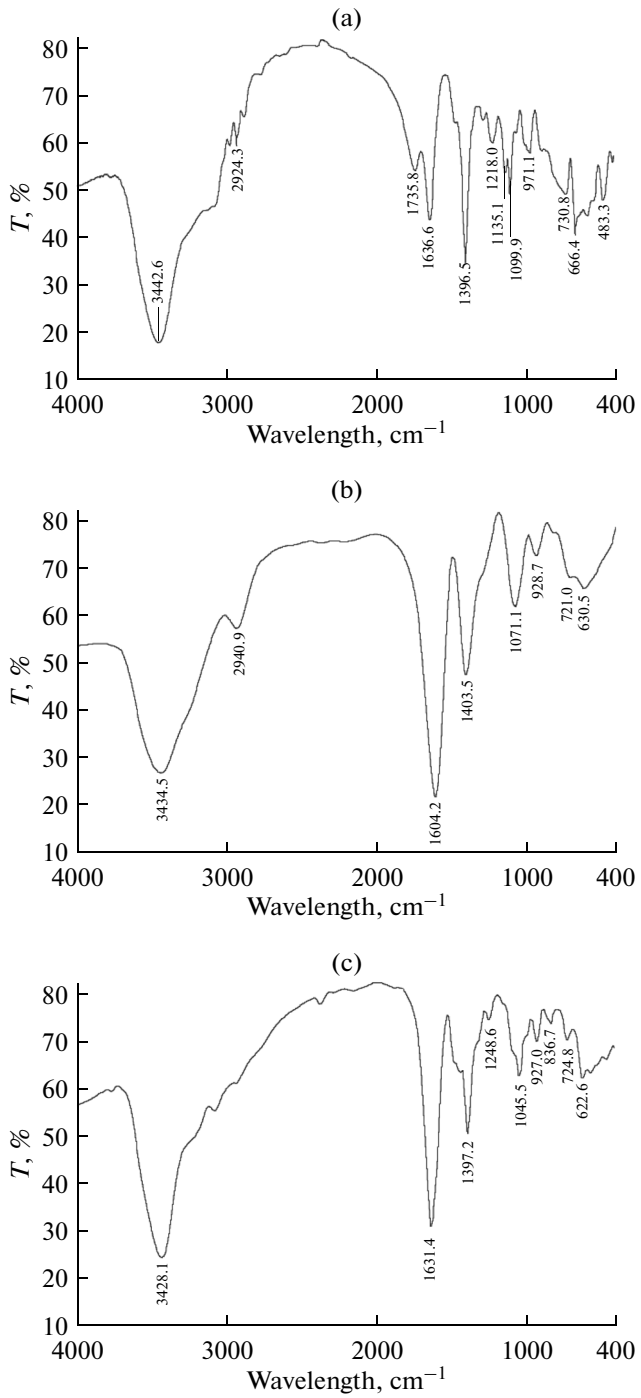

Fig. 1. IR spectra of H_4Egta (a), $\{K[Sm^{III}(Egta) \cdot H_2O\}_n$ (**I**) (b) and $(NH_4)[Lu^{III}(Egta)] \cdot H_2O$ (**II**) (c).

Ltd., China) (0.8718 g, 2.5 mmol) was added slowly to the above solution. The solution became transparent after the mixture had been stirred and refluxed for 15.0 h, and then pH value was adjusted to 5.5 by dilute $KCHO_3$ aqueous solution. Finally, the solution was concentrated to 25 mL. A yellow crystal appeared after three weeks at room temperature. The yield was 2.49 g. (85.17%).

Synthesis of II. H_4Egta (1.9017 g, 5.0 mmol) was added to 100 mL warm water and Lu_2O_3 powder (99.999%, Yuelong Rare Earth Co., Ltd., China) (0.9948 g, 2.5 mmol) was added to above solution slowly. The solution became transparent after the mixture had been stirred and refluxed for 16.0 h. And then the pH value was also adjusted to 5.5 by dilute NH_3 aqueous solution. Finally, the solution was concentrated to 25 mL. A yellow crystal appeared after three weeks at room temperature. The yield was 2.45 g. (83.52%)

X-ray structure determination. X-ray intensity data of **I** and **II** samples were collected on a Bruker SMART CCD type X-ray diffractometer system with graphite-monochromatized MoK_α radiation (λ = 0.71073 Å) at 293(2) K using φ–φ scan technique in the range of $1.72° \le \theta \le 26.00°$. Their structures were solved by direct methods. All non-hydrogen atoms were refined anisotropically by full-matrix least-squares methods. All the calculations were performed by the SHELXTL-97 program on PDP11/44 and Pentium MMX/166 computers. The crystal data and structure refinement for two complexes were listed in Table 1. And the selected bond distances and bond angles of two complexes were listed in Table 2.

Supplementary material has been deposited with the Cambridge Crystallographic Data Centre (nos. 966211 (**I**) and 966210 (**II**); deposit@ccdc.cam.ac.uk or http://www.ccdc.cam.ac.uk).

RESULTS AND DISCUSSION

FT-IR spectra of H_4Egta, complexes **I** and **II** are shown in Fig. 1. As can be seen from the Fig. 1b, there are obvious differences between the FT-IR spectra of H_4Egta ligand and complex **I** on account of coordination reaction of the Sm^{3+} ion and Egta ligand. IR spectrum of complex I indicates that the characteristic peaks of ν(C–N) of complex **I** are at 1071 cm^{-1}, and red shifts are 28 cm^{-1} compared with that of the Egta ligands (1099 cm^{-1}), which demonstrates that the N atoms from Egta ligands are coordinated to the central Sm^{3+} ions. The ν_{as}(COOH) of H_4Egta was disappeared completely, suggesting that all the carboxylic group were coordinated with Sm^{3+}, there is no free carboxylic in group complex. In addition, it can be seen that ν_{as}(COO) at 1637 cm^{-1} of H_4Egta red-shifts to 1604 cm^{-1} in the complex and ν_s(COO) at 1396 cm^{-1} of H_4Egta blue-shifts to 1404 cm^{-1} in the spectrum of the complex, which confirms that the O atoms from carboxylic groups and ether groups also coordinate with the central Sm^{3+} ion. Furthermore, the FT-IR spectra of complex **I** displays a broad absorption band around 3434 cm^{-1}. It could be attributed to the stretching vibration absorption peak of O–H bond. These analytical date show that a new complex gener-

Table 1. Crystallographic data and structure refinement for **I** and **II**

Parameter	Value	
	I	**II**
Empirical formula	$C_{14}H_{23}KN_2O_{11}Sm$	$C_{14}H_{26}N_3O_{11}Lu$
Formula weight	584.79	587.35
Crystal system	Monoclinic	Monoclinic
Space group	$C2/c$	$P2_1/c$
Unit cell dimensions:		
a, Å	38.253(3)	13.9817(10)
b, Å	13.7769(11)	9.7392(6)
c, Å	8.7652(7)	14.6305(13)
β, deg	100.696(2)	110.267(9)
Volume, Å^3	4539.0(6)	1868.9(2)
Z	8	4
ρ_{calcd}, Mg/m^3	1.712	2.087
Absorption coefficient, mm^{-1}	2.824	5.349
F(000)	2320	1160
Crystal size, mm	0.18 × 0.15 × 0.09	0.45 × 0.40 × 0.31
θ Range for data collection, deg	2.96–25.02	2.56–25.02
Limiting indices	$-45 \le h \le 44$	$-16 \le h \le 16$
	$-16 \le k \le 16$	$-11 \le k \le 10$
	$-10 \le l \le 10$	$-17 \le l \le 17$
Reflections collected	3920	12827
Independent reflections, R_{int}	3921 (0.0000)	3299 (0.0710)
Completeness to θ_{max}, %	97.4	100.0
Max and min transmission	0.7852 and 0.6304	0.2879 and 0.1969
Goodness-of-fit on F^2	1.001	1.106
Final R indices, $I > 2\sigma$, I	$R1 = 0.1563$, $wR2 = 0.3754$	$R1 = 0.0406$, $wR2 = 0.0987$
R indices (all data)	$R1 = 0.1798$, $wR2 = 0.4011$	
	$R1 = 0.0494$, $wR2 = 0.1049$	
Largest difference peak and hole, e Å^{-3}	5.785 and −5.552	1.993 and −3.164
Absorption correction	Empirical	
Refinement method	Full-matrix least-squares on F^2	

ated, which are consistent with the result of X-ray diffraction analysis.

From the IR spectrum of complex II in Fig. 1c, it was also found that characteristic peak of ν(C–N) appears at 1046 cm^{-1}, which displays a red-shift (53 cm^{-1}) compared with that (1099 cm^{-1}) of Hegta. This bathochromic shift effect suggested that the N atoms from Egta ligands are coordinated to the central Lu^{3+} ions. The ν_{as}(COO) band of the complex at 1631 cm^{-1} shows a red shift (6 cm^{-1}) compared with 1637 cm^{-1} of the H_4Egta ligand, and ν_s(COO) of complex **II** at 1387 cm^{-1} reveals a red-shift (9 cm^{-1}) compared with 1396 cm^{-1} of the H4Egta ligand. These changes in the peak positions indicate that the oxygen atoms from the carboxyl groups and ether groups are also coordinated to the Lu^{3+} ion. The spectrum of free H_4Egta shows a strong band at 1736 cm^{-1} originating from ν(C=O), which disappears completely in the FT-IR spectrum of **II**. Also the broad absorption of (OH) around 3428 cm^{-1} which could be reasonably assigned to O–H stretch of hydrogen bonds. These analytical date show that a new complex generated, which are consistent with the result of X-ray diffraction analysis.

As seen the TG curve of complex **I** in Fig. 2a, that the first thermal decomposition happens from 25 to 125°C. In this step the weight loss ratio is about 11.04%, which corresponds to the releasing of a crystal water. From 125 to 342°C, there is small weight loss, which means that the crystal structure is stable until

Table 2. Selected bond distances (Å) and angles (deg) of **I*** and **II**

Bond	*d*, Å	Bond	*d*, Å	Bond	*d*, Å
		I			
Sm(1)–O(1)	2.50(2)	Sm(1)–O(5)	2.39(2)	Sm(1)–O(9)	2.44(2)
Sm(1)–O(2)	2.54(2)	Sm(1)–O(7)	2.352(18)	Sm(1)–N(1)	2.61(3)
Sm(1)–O(3)	2.39(2)	Sm(1)–O(8)#1	2.41(2)	Sm(1)–N(2)	2.68(2)
		II			
Lu(1)–O(1)	2.406(5)	Lu(1)–O(5)	2.237(5)	Lu(1)–N(1)	2.447(5)
Lu(1)–O(2)	2.342(5)	Lu(1)–O(7)	2.229(5)	Lu(1)–N(2)	2.494(6)
Lu(1)–O(3)	2.216(5)	Lu(1)–O(9)	2.276(5)		
Angle	ω, deg	Angle	ω, deg	Angle	ω, deg
		I			
O(1)Sm(1)O(2)	66.6(7)	O(2)Sm(1)O(9)	71.4(7)	O(5)Sm(1)N(1)	65.3(9)
O(1)Sm(1)O(3)	98.6(8)	O(2)Sm(1)N(1)	128.6(8)	O(5)Sm(1)N(2)	76.2(7)
O(1)Sm(1)O(5)	126.6(7))	O(2)Sm(1)N(2)	67.0(7)	O(7)Sm(1)O(8)$^{\#1}$	74.4(7)
O(1)Sm(1)O(7)	150.2(8)	O(3)Sm(1)O(5)	79.4(7)	O(7)Sm(1)O(9)	129.3(7)
O(1)Sm(1)O(8)$^{\#1}$	76.2(9)	O(3)Sm(1)O(7)	76.3(7)	O(7)Sm(1)N(1)	132.4(8)
O(1)Sm(1)O(9)	72.6(8)	O(3)Sm(1)O(8)$^{\#1}$	72.1(7)	O(7)Sm(1)N(2)	65.5(7)
O(1)Sm(1)N(1)	65.9(9)	O(3)Sm(1)O(9)	140.5(8)	O(8)$^{\#1}$Sm(1)O(9)	137.3(8)
O(1)Sm(1)N(2)	124.5(7)	O(3)Sm(1)N(1)	64.8(8)	O(8)$^{\#1}$Sm(1)N(1)	115.5(8)
O(2)Sm(1)O(3)	141.5(8)	O(3)Sm(1)N(2)	136.9(8)	O(8)$^{\#1}$Sm(1)N(2)	113.5(7)
O(2)Sm(1)O(5)	138.5(7)	O(5)Sm(1)O(7)	81.9(7)	O(9)Sm(1)N(1)	76.8(8)
O(2)Sm(1)O(7)	98.9(6)	O(5)Sm(1)O(8)$^{\#1}$	146.3(7)	O(9)Sm(1)N(2)	65.1(7)
O(2)Sm(1)O(8)$^{\#1}$	69.9(7)	O(6)Sm(1)O(9)	76.4(7)	N(1)Sm(1)N(2)	131.0(9)
		II			
O(1)Lu(1)O(2)	67.43(16)	O(2)Lu(1)O(9)	92.72(19)	O(5)Lu(1)N(1)	70.78(18)
O(1)Lu(1)O(3)	137.30(17)	O(2)Lu(1)N(1)	137.66(17)	O(5)Lu(1)N(2)	148.01(19)
O(1)Lu(1)O(5)	77.11(17)	O(2)Lu(1)N(2)	72.67(18)	O(7)Lu(1)O(9)	137.65(16)
O(1)Lu(1)O(7)	136.93(17)	O(3)Lu(1)O(5)	104.10(18)	O(7)Lu(1)N(1)	132.31(18)
O(1)Lu(1)O(9)	72.36(16)	O(3)Lu(1)O(7)	83.28(17)	O(7)Lu(1)N(2)	69.93(19)
O(1)Lu(1)N(1)	70.65(17)	O(3)Lu(1)O(9)	85.53(18)	O(9)Lu(1)N(1)	79.99(18)
O(1)Lu(1)N(2)	120.98(19)	O(3)Lu(1)N(1)	69.79(18)	O(9)Lu(1)N(2)	67.98(18)
O(2)Lu(1)O(3)	151.76(17)	O(3)Lu(1)N(2)	80.63(18)	N(1)Lu(1)N(2)	137.77(19)
O(2)Lu(1)O(5)	94.12(18)	O(5)Lu(1)O(7)	79.13(17)		
O(2)Lu(1)O(7)	79.14(18)	O(5)Lu(1)O(9)	143.20(16)		

* Symmetry codes: $^{\#1}$ $x, -y + 1, z - 1/2$.

342°C. From 342 to 451°C, the decomposition and combustion of aminocarboxylate, carboxylate and carbonate take place. In this step the weight loss ratio is about 41.54%. It is estimated that remainder is a Sm_2O_3–$Sm_2(CO_3)_3$ mixture. The total mass loss is 52.58% according to the mass calculation. The TG curve is consistent with the result of X-ray diffraction analysis.

The TG curve of complex **II** in Fig. 2b, roughly shows a three stage decomposition pattern. The first stage weight loss starting from room temperature to 166°C results from the expulsion of ammonia molecule. The weight loss ratio is about 4.0%. From 166 to 257°C, there is small weight loss, which means that the crystal structure is stable until 257°C. The second weight loss of 5.98% from 257 to 300°C should correspond to the crystal water molecules. The third weight loss is attributed to the decomposition of organic ligand starting from 300 to 489°C; the weight loss ratio is 39.97%. It is estimated that, the main species is

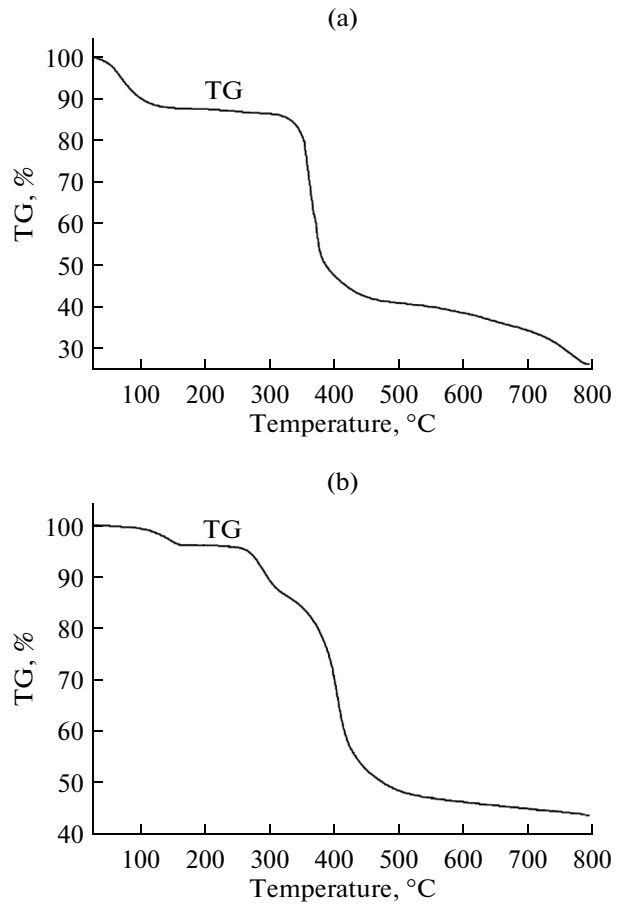

Fig. 2. TG-DTA curve of **I** (a) and **II** (b).

Lu_2O_3 in the remainder, and there is still a little $Lu_2(CO_3)_3$ left. The total weight loss ratio is about 49.95% according to the mass calculation. The TG curve is consistent with the result of X-ray diffraction analysis.

Figure 3a exhibits that I has a nine-coordinated structure. The central Sm^{3+} ion is coordinated by two nitrogens and six oxygens from one octadentate Egta ligand. Meanwhile, one oxygen comes from one carboxylic group of the neighboing Egta ligand. In a part of the asymmetry unit, a carboxyl group bridges two complexes and the rest parts can be arranged by analogy yielding a polynuclear molecule. It should be noticed that the structure is similar to the some previously findings, for example, $\{K[Y^{III}(Egta)_4H_2O\}_n$, $(MnH)_2[Eu^{III}(Egta)]_2 \cdot 6H_2O$ and $(EnH_2)_2[Ho^{III}(Egta)(H_2O)]_2$ complexes, which have been reported to show polynuclear molecular structures. The central Sm^{3+} ion is in a nine-coordinated environment with four carboxyl oxygens (O(3), O(5), O(7) and O(9)), two amine nitrogens (N(1) and N(2)), and two ethylene glycol oxygens (O(1) and O(2)) from one octadentate H_4Egta ligand. The remaining oxygen atom comes from carboxylic group ($O(8)^{\#}$–$C(11)^{\#}$–$O(7)^{\#}$) of the neighboing Egta ligand which connects two neighboring Sm^{3+} ions.

As seen from Fig. 4a, the coordination sphere around Sm^{3+} ion yields a slightly distorted nine-coordinate MC-SAP structure, in which the top and bottom planes are defined by the set ethylene glycol O(1), three carboxyl oxygens O(3), O(5), O(9) and the set of ethylene glycol O(2), two carboxyl oxygens O(7), $O(8)^{\#}$ and N(2), respectively. The ninth atom N(1) is above the plane formed by O(1), O(3), O(5) and O(9) which occupied the capping position. In the top approximate square plane, the dihedral angle between O(5)O(3)O(1) and O(1)O(5)O(9) is 12.88°, and between O(3)O(9)O(5) and O(3)O(9)O(1) is 13.34°. In the bottom quadrilateral plane, the dihedral angle

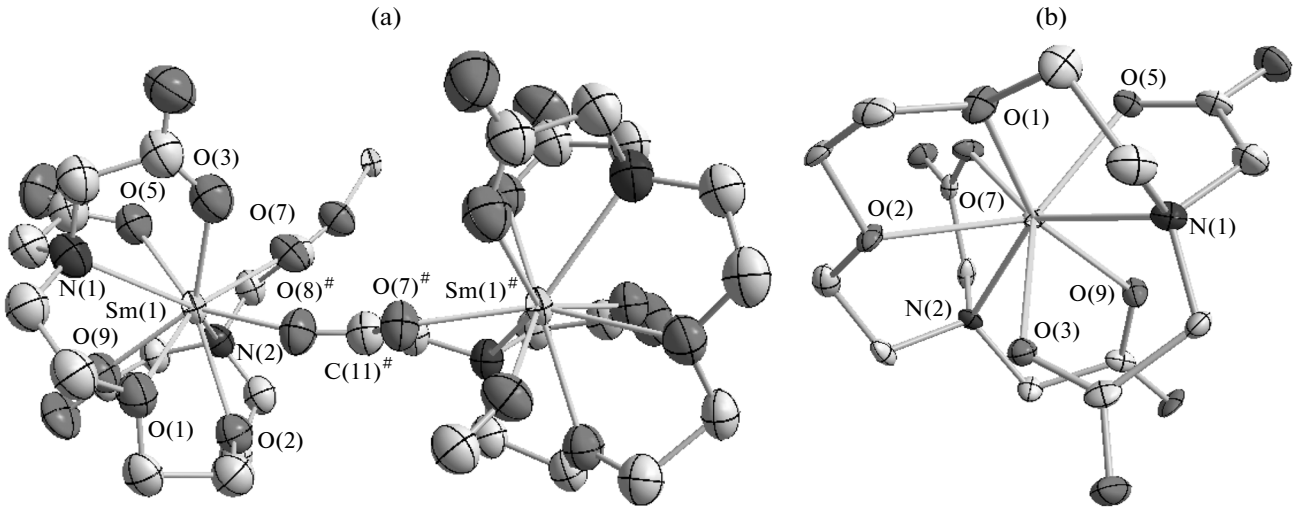

Fig. 3. Molecular structures of **I** (a) and **II** (b).

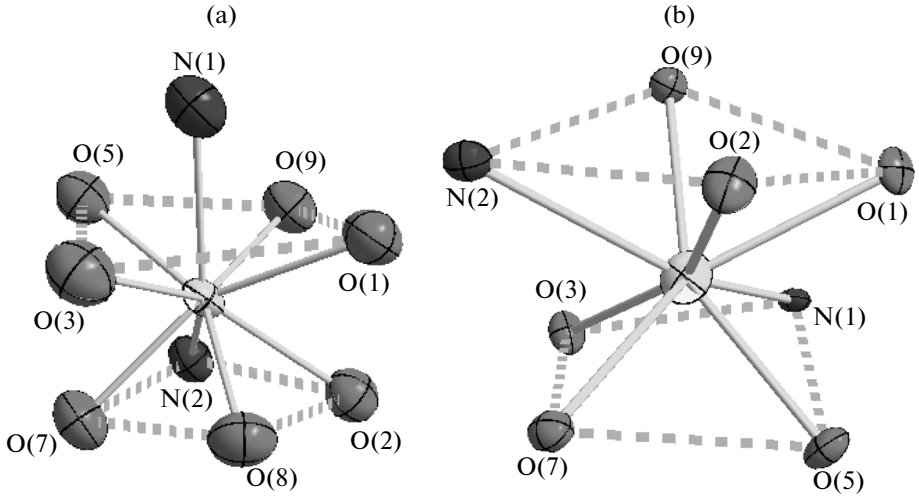

Fig. 4. Coordination polyhedrons around Sm^{3+} ion in **I** (a) and around Lu^{3+} ion in **II** (b).

between N(2)O(7)O(8)$^{\#}$ and N(2)O(2)O(8)$^{\#}$ is 11.38°, and between O(7)O(2)N(2) and O(7)O(2)O(8)$^{\#}$ is 9.94°. According to viewpoints of Guggenberger and Muetterties [26], if the dihedral angle for nine-coordinate rare earth metal complexes is between 0° and 26.4° then their structures are regarded as monocapped square antiprismatic. So we can firmly conclude that the geometry conformation of complex I adopts monocapped square antiprismatic. Futhermore, the average value of the angles (O(1)Sm(1)N(1)), (O(3)Sm(1)N(1)), (O(5)Sm(1)N(1)), and (O(9)Sm(1)N(1)) is 68.2°, in which the biggest and smallest angles are 76.8° and 64.8°, respectively. Obviously, it is close to 70° that most complexes with nine-coordinate monocapped square antiprismatic structures keep. According to these dates, it proves again that complex I distorts a little as a standard monocapped square antiprismatic.

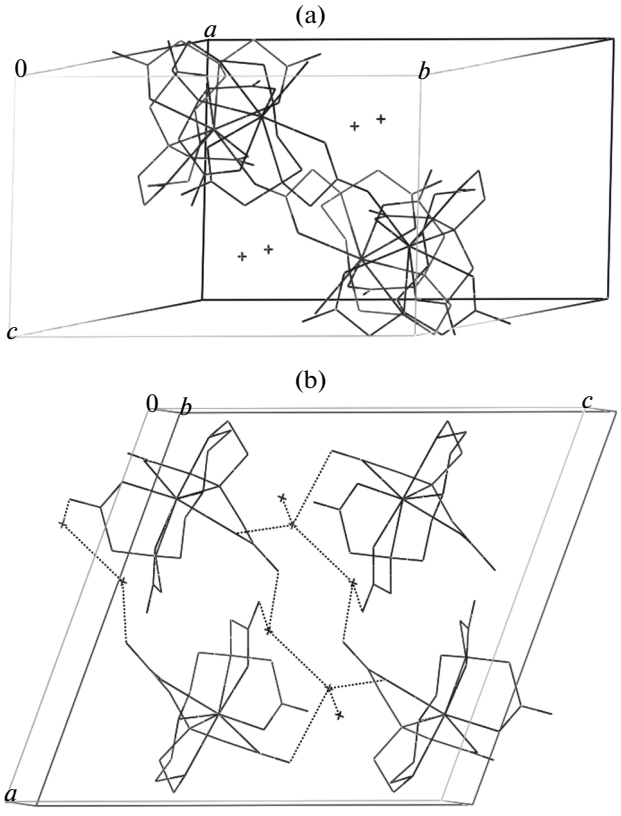

Fig. 5. Arrangements of **I** (a) and **II** (b) in unit cell (dashed lines represent intermolecular hydrogen bonds).

In addition, as shown in Table 2, the lengths of the Sm(1)-O bond in complex I have a wide range from 2.35(18) Å (Sm(1)–O(7)) to 2.54(2) Å (Sm(1)–O(2)), and the average is 2.43(4) Å. Among these Sm–O bonds, Sm(1)–O(1) and Sm(1)–O(2) (belonging to ethylene glycol oxygens) are longer than other Sm(1)–O bond lengths which illustrates they are affected by the tension from two adjacent five-memberd rings, and this phenomenon is accordance with previously reported H_4Egta. On the one hand, the Sm(1)–O(8)$^{\#}$ (from a carboxyl group of the adjacent Egta ligand) bond distance (2.41(2) Å) is relatively short among other Sm(1)–O bond distances, which demonstrates that the bond Sm(1)–O(8)$^{\#}$ is stable enough. On the other hand, the Sm–N bond lengths range between 2.61(3) Å (Sm(1)–N(1)) and 2.68(2) Å (Sm(1)–N(2)) with an average value of 2.65(2) Å. The average value of Sm–N (2.64 Å) bond lengths is much longer than the mean value of Sm–O (2.43 Å) bond lengths, which firmly indicates that O atoms coordinate to the central Sm^{3+} ion much stronger than N atoms coordinate to Sm^{3+} ion. So it is obviously to conclude that the Sm(1)–O bonds are much more stable than the Sm(1)–N bonds. Among the smallest and largest bond angles are 64.8(8)° (O(3)Sm(1)N(1)) and 150.2(8)° ((O(1)Sm(1)O(7)), respectively.

As seen from Fig. 5a, there are four molecules in one unit cell of complex I. The complex molecules connect with another by sharing the same carboxyl group, electrostatic forces and potassium cations. The potassium cations link to each other with crystallization water, which contribute to stabilizing the crystal structure. The potassium cation connects with three adjacent $[Sm^{III}(Egta)]^-$ complex anions. Each potassium cation is eight-coordinate by eight coordinate carboxylic O atoms: O(3), O(4), O(5) and O(7) (all from one ligand), one non-coordinate carboxylic O(4) atom (from another adjacent Egta), O(3) and O(4) atoms (from the third adjacent Egta) and O(11) atom (from crystal water molecules). The K^+ ions link the chains to form a layer structure. Thus, the electrostatic forces play an important role in the structure of complex **I**.

Evidently, in crystal structure **II**, the Lu^{3+} cation forms a eight-coordinated 1:1 complex with H_4Egta in Fig. 3b. The central Lu^{3+} ion is coordinated with four carboxyl O atoms (O(3), O(5), O(7) and O(9)), two ethylene glycol O atoms (O(1) and O(2)), two amine N atoms (N(1) and N(2)) from only one octadentate H_4Egta ligand without coordinated water in a SAP structure. This coordination structure forms seven five-membered chelating rings. We learn from intrinsic laws and experiences that the coordinate structure and coordination number of lanthanide complexes are relate to its rare earth ionic radius and electronic configuration. This study again proves that the sizes of rare earth metal ionic radius and electronic configuration have a great effect on the coordinate structure and coordination number of lanthanide complexes.

As seen from Fig. 4b, the coordination polyhedron of the $Lu^{III}N_2O_6$ moiety in complex **II** adopts a eight-coordinate SAP structure, in which the set of O(1), O(2), O(9) and N(2) and the set of O(3), O(5), O(7) and N(1) compose two approximately parallel square planes. There is no capped atom in the geometric configuration of this complex, which means no repulsion to the top or bottom square plane could yield. The dihedral angle between N(2)O(2)O(9) and O(1)O(2)O(9) is 20.65°, and between N(2)O(1)O(2) and N(2)O(1)O(9) is 26.17° in the top approximate square plane. The dihedral angle between O(7)O(3)O(5) and N(1)O(3)O(5) is 21.47°, and between O(7)N(1)O(3) and O(7)N(1)O(5) is 25.91° in the bottom quadrilateral plane. All the data above confirm that the coordination geometry of complex II distorted slightly as a standard SAP conformation.

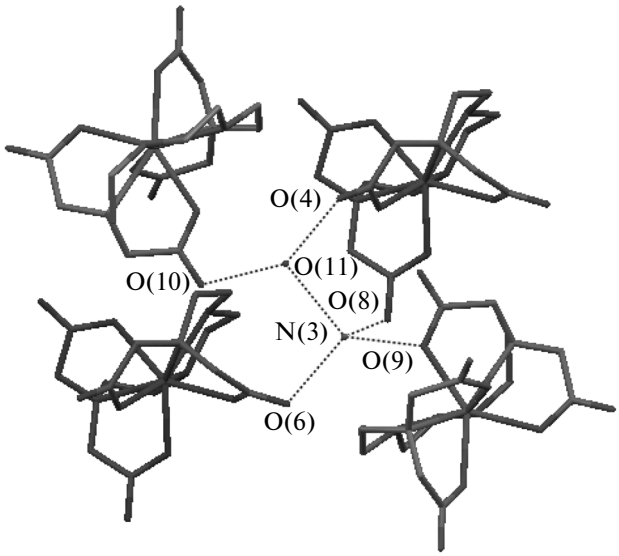

Fig. 6. Bindings between NH_4^+ and $[Lu^{III}(Egta)]^-$ in **II** (dashed lines represent intermolecular hydrogen bonds).

For complex II, the Lu(1)–O bond distances vary from 2.406(5) Å (Lu(1)–O(1)) to 2.216(5) Å (Lu(1)–O(3)) with the average value of 2.284(5) Å. The Lu(1)–N bond distances range from 2.494(6) Å (Lu(1)–N(2)) to 2.447(5) Å (Lu(1)–N(1)) with the average value of 2.471(8) Å, which are significantly longer than the Lu(1)–O bond distances. As a general rule, it indicates that the Lu(1)–O bonds are much stronger than the Lu(1)–N bonds. Table 2 also illustrates a series of bond angle. The smallest and largest bond angles are 66.43(16)° (O(1)Lu(1)O(2)) and 151.76(17)° (O(2)Lu(1)O(3)), respectively. The reason might be that the O(2) forms hydrogen bond with the adjacent crystal water.

In one unit cell of complex **II**, there are four complex molecules in Fig. 5b. The molecules connect with crystal water and protonated ammonium cations (NH_4^+) through hydrogen bonds Thus, the hydrogen bonds play an important role in the construction of the

Table 3. Geometric parameters of hydrogen bonds of **II**

D–H...A	Distance, Å			Angle DHA, deg	Symmetry code
	D–H	H...A	D...A		
N(3)–H(3C)...O(6)	0.90	2.09	2.837(5)	139	$x, -y + 1/2, z + 1/2$
N(3)–H(3D)...O(8)	0.90	2.02	2.904(6)	166	$x, -y + 3/2, z + 1/2$
N(3)–H(3E)...O(9)	0.90	2.00	2.893(5)	173	
N(3)–H(3F)...O(11)	0.90	1.89	2.788(7)	172	$x, -y + 1/2, z + 1/2$

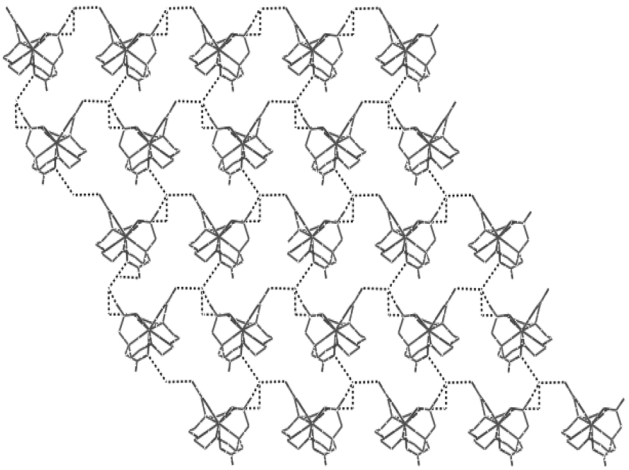

Fig. 7. Polyhedral view of the 1D ladder-like layered network of **II**.

coordinate structure. As shown in Fig. 6 and Table 3, an ammonium cation forms the hydrogen bonds with O(6), O(8) and O(9), from carboxyl O atoms of three neighboring $[Lu^{III}(Egta)]^-$ complexes anions. In addition, ammonium cation connects with of crystal water as well. Meanwhile, the O(10) atoms links to O(10) and O(4), which belong to another adjacent $[Lu^{III}(Egta)]^-$ complex anions and one of above three neighboring $[Lu^{III}(Egta)]^-$ complex anions. The distances of N(3)...O(6), N(3)...O(8), N(3)...O(9) and N(3)...O(11) are 2.837, 2.904, 2.893 and 2.788 Å, forming a 1D chains structure. Figure 6 extends out and forms Fig. 7. 1D chains are linked by sharing NH_4^+ cations, leading to the formation of a 1D ladder-like network.

ACKNOWLEDGMENTS

The authors greatly acknowledge the National Science Founda-tion of China (21371084), Innovation Team Project of Education Department of Liaoning Province (LT2012001), Public Research Fund Project of Science and Technology Department of Liaoning Province (2012004001), Shenyang Science and Technology Plan Project (F12-277-1-15 and F13-289-1-00) and Science Foundation of Liaoning Provincial Education Department (L2011007) for financial support. The authors also thank our colleagues and other students for their participating in this work.

REFERENCES

1. Mikhalyova, E.A., Yakovenko, A.V., Zeller, M., et al., *Inorg. Chim. Acta*, 2014, vol. 44, p. 97.
2. Maspoch, D., Molina, D.R., Veciana, J., et al., *Chem. Soc. Rev.*, 2007, vol. 36, p. 770.
3. Manna, S.C., Zangrando, E., Ribas, J., et al., *Polyhedron*, 2006, vol. 25, p. 1779.
4. Matsumiya, H., Inoue, H., and Hiraide, M., *Talanta*, 2014, vol. 128, p. 500.
5. Ratanajanchai, M., Lee, D.H., Sunintaboon, P., et al., *J. Colloid. Interf. Sci.*, 2014, vol. 415, p. 70.
6. Cho, I., Kang, J.G., and Sohn, Y., *J. Lumin.*, 2015, vol. 157, p. 264.
7. Elistratova, J., Burilov, V., Mustafina, A., et al., *Colloids Surf., A*, 2015, vol. 457, p. 402.
8. Liu, R., Yang, J., and Wu, X., *J. Lumin.*, 2002, vol. 96, p. 201.
9. Richardson, F.R., *Chem. Rev.*, 1982, vol. 82, p. 541.
10. Lima, L.M.P., Delgado, R., Marques, F., et al., *Eur. J. Med. Chem.*, 2010, vol. 45, p. 5621.
11. Ouadi, A., Bultel, K., France-Robert, A.D., et al., *Tetrahedron Lett.*, 2004, vol. 45, p. 1395.
12. Ouadi, A., Loussouarn, A., Morandeau, L., et al., *Eur. J. Med. Chem.*, 2004, vol. 39, p. 467.
13. Faridbod, F., Sedaghat, M., and Hosseini, M., *et at., Spectrochim. Acta, A*, 2015, vol. 117, p. 1231.
14. Bozoglu, C. Erdogmus, A., et al., *Electrochim. Acta*, 2013, vol. 113, p. 668.
15. Zugle, R., Antunes, E., Khene, S., et al., *Polyhedron*, 2012, vol. 33, p. 74.
16. Das, T., Chakraborty, S., Banerjee, S., et al., *Appl. Radiat. Isot.*, 2007, vol. 65, p. 301.
17. Ranjbar, H., Ghannadi-Maragheh, M., Bahrami-Samani, A., et al., *Radiat. Phys. Chem.*, 2015, vol. 108, p. 60.
18. Neves, M., Gano, L., Pereira, N., et al., *Nucl. Med. Biol.*, 2002, vol. 29, p. 329.
19. Gao, J.Q., Dan, L., Wang, J., et al., *J. Coord. Chem.*, 2011, vol. 37, p. 817.
20. Ma, C.C., Li, Y., Wang, J., et al., *J. Coord. Chem.*, 2013, vol. 66, p. 3660.
21. Chen, X., Li, D., Wang, J., et al., *J. Coord. Chem.*, 2010, vol. 63, p. 3897.
22. Gao, J.Q., Wu, T., Wang, J., et al., *Russ. J. Coord. Chem.*, 2011, vol. 37, p. 817.
23. Zhang, L.Q., Fan, T.T., Wang, J., et al., *Russ. J. Coord. Chem.*, 2010, vol. 36, p. 819.
24. Bai, Y., Gao, J.Q., Wang, J., et al., *Russ. J. Coord. Chem.*, 2013, vol. 39, p. 147.
25. Wang, J., Zhang, X.D., and Liu, Z.R., *J. Mol. Struct.*, 2002, vol. 613, nos 1-3, p. 189.
26. Guggenberger, L.J. and Muetterties, E.L., *J. Am. Chem. Soc.*, 1976, vol. 98, p. 7221.